Enhanced Photon Generation in a Nb/$n-$InGaAs/$p-$InP Superconductor/Semiconductor-Diode Light Emitting Device

H. Sasakura,[1,2,*] S. Kuramitsu,[1,3] Y. Hayashi,[1] K. Tanaka,[2,4] T. Akazaki,[2,5] E. Hanamura,[6] R. Inoue,[2,7] H. Takayanagi,[2,7,8] Y. Asano,[9] C. Hermannstädter,[1] H. Kumano,[1,2] and I. Suemune[1,2,†]

[1]*Research Institute for Electronic Science, Hokkaido University, Sapporo 001-0021, Japan*
[2]*CREST, Japan Science and Technology Agency, Kawaguchi 332-0012, Japan*
[3]*Graduate School of Information Science Technology, Hokkaido University, Sapporo 060-0814, Japan*
[4]*Central Research Laboratory, Hamamatsu Photonics, Hamamatsu 434-8601, Japan*
[5]*NTT Basic Research Laboratory, Atsugi 243-0198, Japan*
[6]*Japan Science and Technology Agency, Kawaguchi 332-0012, Japan*
[7]*Department of Applied Physics, Tokyo University of Science, Tokyo 162-8601, Japan*
[8]*International Center for Materials Nanoarchitectonics, NIMS, Tsukuba 305-0044, Japan*
[9]*Graduate School of Engineering, Hokkaido University, Sapporo 060-8628, Japan*

(Received 27 October 2009; revised manuscript received 23 August 2010; published 6 October 2011)

We experimentally demonstrate Cooper pairs' drastic enhancement of the band-to-band radiative recombination rate in a semiconductor. Electron Cooper pairs injected from a superconducting electrode into an active layer by the proximity effect recombine with holes injected from a p-type electrode. The recombination of a Cooper pair with p-type carriers dramatically increases the photon generation probability of a light-emitting diode in the optical-fiber communication band. The measured radiative decay time rapidly decreases with decreasing temperature below the superconducting transition temperature of the niobium electrodes. Our results indicate the possibility to open up new interdisciplinary fields between superconductivity and optoelectronics.

DOI: 10.1103/PhysRevLett.107.157403 PACS numbers: 78.60.Fi, 74.25.Gz, 78.66.Fd, 85.60.Jb

Recent discoveries of new superconductors [1,2] boosted up the research fields with new experimental as well as theoretical possibilities. From a scientific viewpoint one great advantage of superconductivity is its long coherence time which is the most important feature for quantum information processing [3]. The combined system consisting of a coherent photon field and a superconducting (SC) condensate would be a promising candidate for realizing the quantum operation in solid state devices [4–8]. The Cooper pairs are preserved during these operations with photon energies smaller than the energy gap of superconductivity (on the order of meV). On the other hand, when photon energies become larger than the superconductivity gap, the absorption of high-energy photons only results in the destruction of Cooper pairs. This fact enables the application of superconductors as high-speed single-photon detectors [9]. It is still unexplored what will take place with the counter process of photon emission from Cooper-pair states in this higher photon energy range.

In this Letter, we demonstrate that electron Cooper pairs injected into a semiconductor by the proximity effect [10,11] can be highly involved in the interband transition and accelerate the photon generation processes. We measure the radiative recombination rate as a function of temperature across the SC transition temperature, T_C. The results demonstrate drastic enhancement of the radiative recombination rate below T_C. The temperature dependence of the radiative recombination rate can be explained by a theoretical model. Our new finding corresponds to experimental demonstration of the Cooper pair's gigantic oscillator strength [12].

The light-emitting diode (LED) epitaxial layers were grown on a p-type (001) InP substrate by metalorganic vapor-phase epitaxy. The layers consist of a 500 nm thick p^+-InP buffer layer (Zn doping $\sim 1\times 10^{17}$ cm^{-3}), a 30 nm thick n^+-In$_{0.53}$Ga$_{0.47}$As active layer (Si doping $\sim 5\times 10^{18}$ cm^{-3}) lattice matched to InP, and a 10 nm thick n^+-In$_{0.7}$Ga$_{0.3}$As Ohmic contact layer (Si doping $\sim 5\times 10^{18}$ cm^{-3}). Outside of the contact layer, we attached 20 μm wide and 80 nm thick niobium (Nb) electrodes. A 110 nm wide slit was fabricated by reactive ion etching of the Nb as shown in Fig. 1(b). The p electrode was formed with Au/Cr metal layers and was used as the anode for the LED operation as well as the back gate for the Nb/$n-$InGaAs/Nb I-V measurements. When the LED is forward biased across the p-n junction with the common voltage to the split Nb electrodes, electron Cooper pairs are injected into the 40 nm deep $n-$InGaAs/$p-$InP junction through the conduction band of the $n-$InGaAs layers and recombine with holes in the valence band injected from the counter p-type electrode through the $p-$InP substrate [Fig. 1(c)]. The LED was set in a ^{3}He closed-cycle cryostat equipped with optical fibers. After passing through the slit, electroluminescence (EL) was directly collected by a multimode optical fiber with a core diameter of 200 μm located $\sim$0.5 mm above the slit [Fig. 1(a)].

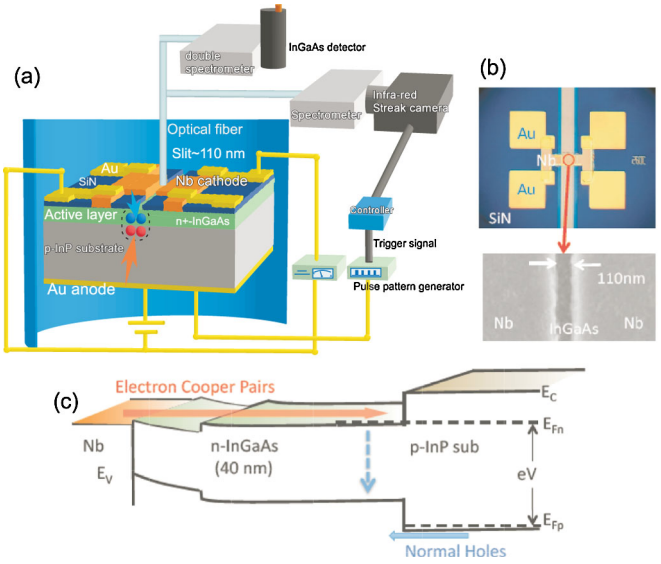

FIG. 1 (color online). Cooper-pair LED and measurement setup: (a) Schematic illustration of the LED structure and measurement setup of the I-V and EL properties. (b) Optical-microscope picture of the LED surface and the expanded secondary-electron-microscope picture of the slit formed in the niobium (Nb) electrode. (c) Schematic diagram of electron Cooper-pair injection from the surface Nb electrodes to the p-n junction, which recombine with holes in the valence band injected with the higher forward bias of the p electrode.

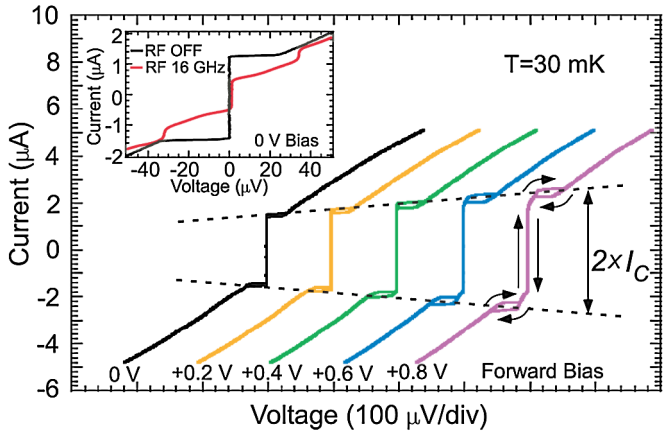

FIG. 2 (color online). Current-voltage characteristics of the Nb/n − InGaAs/Nb junction on the LED surface measured at 30 mK. The inset data were measured at 16 GHz; however, the Shapiro step intervals change with $\Delta V = 2.1\ \mu$V/GHz by changing the RF. The I-V characteristics with the different forward bias are all offset by 100 μV for clarity.

The Cooper-pair injection into the InGaAs semiconductor is examined by measuring the current-voltage (I-V) characteristics between the two Nb SC electrodes on the LED surface [Fig. 1(b)]. The I-V characteristics show typical features of a Josephson junction (critical supercurrent of $I_C \sim 1.2\ \mu$A) and Shapiro steps [13] under the application of a radio-frequency (RF) signal (inset of Fig. 2). That is, the two Nb electrodes together with the n − InGaAs between them form a superconductor/semiconductor/superconductor (S/Sm/S) junction, and Cooper pairs carry supercurrent across the S/Sm/S junction. In addition, we found that the Josephson junction characteristics depend on the forward bias applied to the p-n junction (Fig. 2). When the current flowing through the p-n junction is negligible, I_C increases with the forward bias. The increase of the critical supercurrent is attributed to the increase of the n − InGaAs channel width in the Josephson junction, which is modulated by the thickness of the depletion layer in the n − InGaAs side of the p-n junction. These experimental results strongly indicate that the Cooper pairs injected from one side of the Nb electrode [in Fig. 1(b)] pass through the light-emitting layer very close to the p-n junction to the other side.

In Fig. 3(a) we show a typical EL spectrum observed with forward bias of the p-n junction at 4 K under a constant electric current of 250 μA. The emission peak photon energy of 0.86 eV (1.44 μm wavelength) is in the optical-fiber communication band. The photon energy is determined by the energy gap of InGaAs lattice-matched to InP and n-type doping in the light-emitting layer. The influence of the Cooper pairs on the LED operation can be most efficiently visualized by decay time measurements of the EL intensity. For this purpose the injection current was stepwise decreased from the steady-current ON state to the offset-biased OFF state as shown in the inset of Fig. 3(b), and the resultant transient EL decay was examined. The ON-state diode current was set constant to 250 μA and the OFF-state offset bias was set to 600 mV. The latter offset bias was selected to satisfy both the negligible diode current of less than 1 nA and the negligible internal-field effect based on a series of measurements on the bias dependence. Measurement data obtained at 10 K is shown in the inset of Fig. 3(b) [open (blue) circles]. Since our LED in the cryostat is connected with an external pulse generator and DC bias circuits via a coaxial cable and wires, the current pulse injected into the LED shows the circuit capacitance-resistance (CR) time delay. Assuming the current switching from the steady state to turned off as shown in the inset of Fig. 3(b), the transient decay of the spectrally integrated EL intensity for $t \geq 0$ is given by

$$I_{\mathrm{EL}}(t) = J_0 \eta_{\mathrm{int}} \eta_{\mathrm{det}} \{ e^{-t/\tau_{\mathrm{LED}}} + (1 - \tau_{\mathrm{LED}}/\tau_{\mathrm{CR}})^{-1} \times (-e^{-t/\tau_{\mathrm{LED}}} + e^{-t/\tau_{\mathrm{CR}}}) \}, \quad (1)$$

where τ_{LED}, τ_{CR}, J_0, η_{int}, and η_{det} are the EL decay time constant, the system CR time constant, the injection current divided by the electric charge, the LED internal quantum efficiency, and the EL detection efficiency, respectively. This equation is simplified to the single exponential form of $I_{\mathrm{EL}}(t) = J_0 \eta_{\mathrm{int}} \eta_{\mathrm{det}} e^{-t/\tau_{\mathrm{CR}}}$ under the condition of $\tau_{\mathrm{LED}} \ll \tau_{\mathrm{CR}}$. This single exponential decay is realized when the offset bias is changed to zero [solid

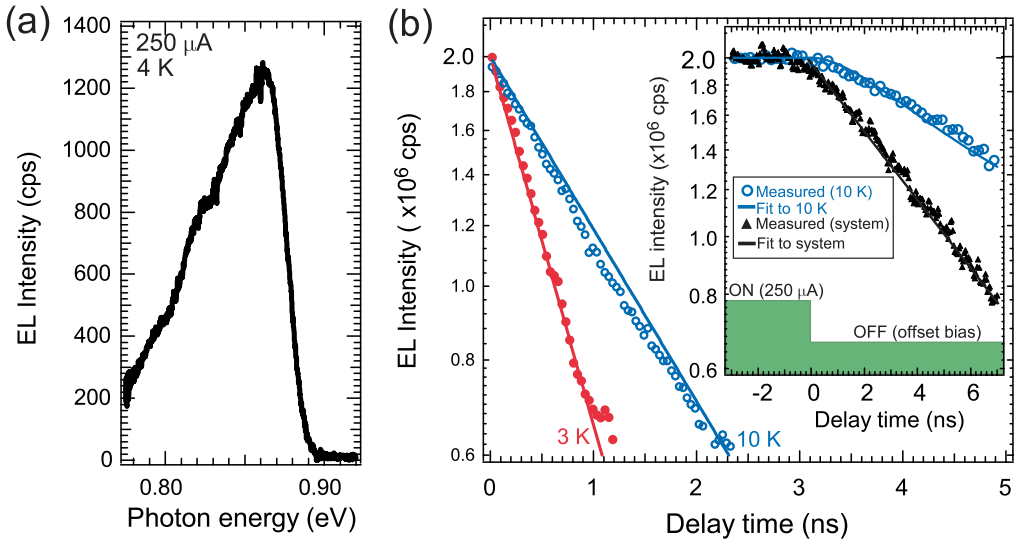

FIG. 3 (color online). (a) EL spectrum measured at 4 K with constant injection current. (b) Transient decay of the spectrally integrated EL intensity: the diode bias set to the ON state is stepwise changed to the OFF state at 0 ns. The measured transient EL decay is shown in the inset with the offset bias of zero and 600 mV shown with solid (black) triangles and open (blue) circles, respectively. The solid lines are the model fitting. The intrinsic EL transients restored from the measured data are shown for 3 and 10 K.

triangles in the inset of Fig. 3(b)]. The shortening of τ_{LED} is attributed to the internal-electric-field-induced Stark effect that spatially separates electrons and holes [14]. The fit shown with a solid line determines τ_{CR} to be 2.70 ns. Then, from the fit to the 10 K data [solid (blue) line], τ_{LED} is determined to be 2.27 ns. Once the time constants are fixed in this way, the intrinsic EL time decay can be restored from the measured EL intensities at 10 K and is reproduced in Fig. 3(b). The comparison between the EL transients at 10 and 3 K demonstrates the clear reduction of decay time for the lower temperature.

Figure 4(a) shows the temperature dependence of τ_{LED}. The measured decay times of a reference LED without SC electrodes [open (blue) triangles] were almost constant in this temperature range. However, an abrupt change of τ_{LED} was observed in the Cooper-pair LED [solid (red) circles]. τ_{LED} at the temperature above ~7.5 K is constant and corresponds to τ_{LED}~2.25 ns of the reference LED, whereas it decreases abruptly below T_{C}. At 0.8 K, τ_{LED} is shortened down to ~1.1 ns. The resistivity of the Nb electrode was measured employing the two neighboring Au pads [Fig. 1(b)] and is shown in Fig. 4(b). It is stepwise

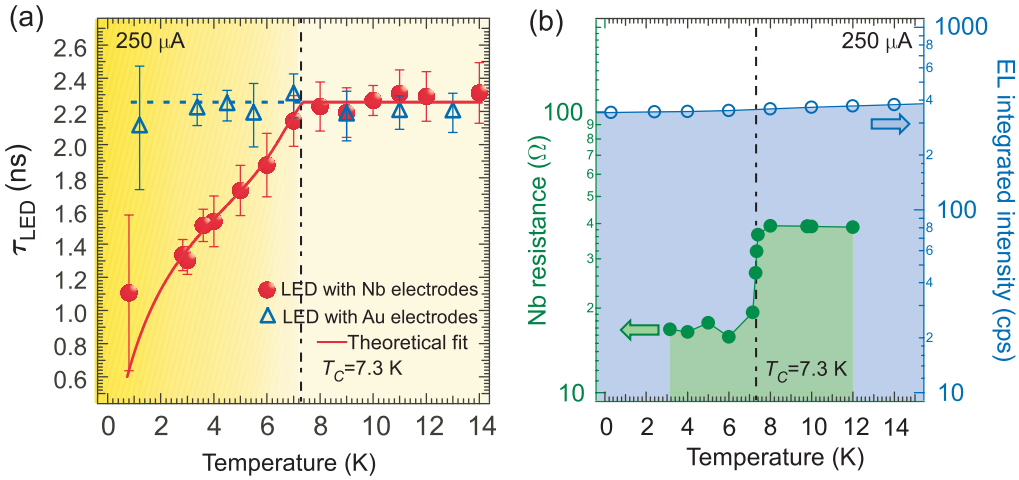

FIG. 4 (color online). (a) Temperature dependence of the measured LED decay time, τ_{LED} [solid (red) circles]; note that the larger error bar at the 0.8 K point is due to the limited measurement time because of heating of the current-driven LED device at the lowest temperatures and the conversion of the cryostat operation mode. The solid (red) line is the fit with Eq. (2). Open (blue) triangles show τ_{rad} of a reference LED device with the electrode material exchanged from Nb to normal metal (Au); the dashed (blue) line is a guide to the eye. (b) The resistance [solid (green) circles] measured along the Nb electrode indicates $T_{\mathrm{C}} = 7.3$ K; the integrated EL intensity [open (blue) circles] during the ON-state shows a temperature independent behavior.

reduced at the temperature of 7.3 K, which indicates $T_C = 7.3$ K in our device [15]. The formation of electron Cooper pairs initiates in the Nb electrode below T_C and the onset temperature of the EL decay time shortening precisely agrees with T_C. This agreement as well as the significant decay time shortening below T_C demonstrates the major role of the injected Cooper pairs for the enhanced recombination rate in the LED.

The LED internal quantum efficiency, η_{int}, is given by the balance of the radiative and nonradiative recombination rates as follows: $\eta_{int} = 1/\tau_{rad}/[1/\tau_{rad} + 1/\tau_{nonrad}]$, where $\tau_{(non)rad}$ is the (non)radiative decay time and $1/\tau_{LED} = 1/\tau_{rad} + 1/\tau_{nonrad}$. The steady-state EL intensity is given by $I_{EL}(t \leq 0) = J_0 \eta_{int} \eta_{det}$. We previously observed drastic EL enhancement below T_C [16] and attributed that to the case of low internal quantum efficiency [17]. In this case $\eta_{int} \ll 1$ or, equivalently, $\tau_{rad} \gg \tau_{nonrad}$ and the EL intensity is given by $I_{EL}(t \leq 0) = J_0 \eta_{int} \eta_{det} \approx J_0 \eta_{det} \tau_{nonrad}/\tau_{rad}(T)$. Therefore, the EL intensity is enhanced with the reduction of the radiative lifetime under constant injection current. In the present case despite the significant change of the measured decay time below T_C, the integrated EL intensities in the steady state remain almost independent of the temperature [open (blue) circles in Fig. 4(b)]. This much different situation can be accounted for by the condition of $\tau_{rad}(T) \ll \tau_{nonrad}$ or equivalently $\eta_{int} = 1/\tau_{rad}(T)/[1/\tau_{rad}(T) + 1/\tau_{nonrad}] \simeq 1$. The EL output under constant injection current is given by $I_{EL} = J_0 \eta_{int} \eta_{det} \simeq$ constant and is therefore independent of the $\tau_{rad}(T)$ decrease.

The number of emitted photons at $t = 0$ is identical comparing the 3 and 10 K data as shown in Fig. 3(b). However, the total number of photons emitted during the decay is reduced to $1.1/2.3 \sim 0.5$ at 3 K compared to 10 K. This is explained by the relation of $J_0 = p_0/\tau_{LED} \approx p_0(T)/\tau_{rad}(T)$, that is, the steady-state hole concentration p_0 is reduced for the shorter τ_{rad} value for $T < T_C$ under constant injection current. The ratio of the measured decay time at 3 and 10 K is $1.4/2.25 \sim 0.6$ and is within the reasonable range to the above ratio of the photon numbers.

The observed drastic change of the photon generation processes was examined with a theoretical model considering Cooper pairs [12,18,19]. Since the InGaAs active layer is highly n-type doped, the τ_{rad} discussed here is for the minority carriers (holes in the valence band). To analyze the experimental data, we apply a phenomenological formula for the inverse lifetime, [expression of Eq. (2)], where we approximately consider the proximity effect through the exponential function in the second term

$$\frac{1}{\tau_{rad}} = \frac{1}{\tau_{rad}^{normal}} + A \frac{\Delta_0^2(T)}{T} \exp\left(-\frac{2L}{\xi_N(T)}\right). \quad (2)$$

The first term is the radiative recombination lifetime related to the normal electron and hole recombination. τ_{rad}^{normal} was measured to be $\sim$2.25 ns from the reference LED with the normal metal (Au) electrode in Fig. 4(a). τ_{rad}^{normal} is generally expressed as $1/BN$, where the B coefficient for the InGaAs active layer has been measured as 1.43×10^{-10} cm^{-3} s^{-1} [20]. N is the majority carrier (electron) concentration and the value corresponding to the measured lifetime is 3.1×10^{18} cm^{-3}. This is close to the donor doping level of $\sim 5 \times 10^{18}$ cm^{-3}. The second term expresses the radiative recombination lifetime related to the electron Cooper-pair recombination in the temperature range below T_C. Essentially the same theoretical term as this second term has been derived with Eq. (23) in Ref. [19] considering the radiative recombination of a Cooper pair in the conduction band and a pair of normal holes in the valence band. $\Delta_0(T)$ is the temperature-dependent superconducting gap [10,11], and L is the distance from the S-Sm interface to the LED active layer which is 40 nm in the present LED. $\xi_N(T)$ is the coherence length of the electron Cooper pairs penetrating into the $n-$ InGaAs active layer and is given by $(\hbar^3 \mu/2\pi k_B T m_e e)^{1/2}(3\pi^2 N_{3D})^{1/3}$ [21], where $\hbar$ and k_B are the Planck constant and the Boltzmann constant. For the $In_{0.53}Ga_{0.47}As$ layer, the electron mobility was assumed to be $\mu \sim 4000$ cm^2/V s based on measurements at 77 K and room temperature. For the electron concentration of $N_{3D} \sim 5 \times 10^{18}$ cm^{-3} and the electron effective mass of $m_e/m_0 = 0.043$ [22], the distance L is much shorter than the calculated coherence length. The constant A is the only one fitting parameter that includes the dipole transition matrix element [19] and this determines the relative contribution ratio of the Cooper pairs and normal electrons.

The solid line in Fig. 4(a) is the fitting of Eq. (2) to the measured lifetime. Although there remain error bars, the measured delicate temperature dependence below T_C is well reproduced with Eq. (2) except for 0.8 K. This is due to technical limitations of our cryostat where the cooling setup changes from conventional pulse-tube refrigerator to a ^{3}He condensation pot. Because of the lower cooling power the limited measurement time resulted in the large error bars. From the lifetime change with the superconductivity, we can derive the ratio of the Cooper pair and normal-electron contributions in the recombination process which are 43% and 57% at 3 K, respectively.

The physics behind this drastic effect of Cooper pairs on the radiative recombination process is attributed to the conversion from Fermionic independent electrons to the Cooper pairs in a BCS condensate. This superconducting condensate in the conduction band enhances the interband radiative recombination probability. EL spectral change related to the superconducting condensate is observable but is bias-dependent in the present LED device, and the details will be reported in a future publication.

In summary, we investigated the recombination of electron Cooper pairs with p-type carriers in the semiconductor LED with superconducting electrodes and compared the results with a theoretical model. Drastic enhancement

of the radiative recombination rate was observed below the superconducting critical temperature of the Nb electrodes. This new finding of the Cooper pair's gigantic oscillator strength in semiconductor interband optical transitions opens up new interdisciplinary fields between superconductivity and optoelectronics.

We thank M. Jo for potential profile calculations of the LED structure, H. Kan and M. Yamanishi for valuable discussion on our measurements. Supports from the Hokkaido Innovation through Nanotechnology Support, Post-Silicon Materials and Devices Research Alliance, and Global COE, Graduate School of IST, Hokkaido University are acknowledged. C. H. acknowledges the Japan Society for the Promotion of Science (JSPS) for providing financial support in the form of a JSPS Fellowship for Foreign Researchers.

*hirotaka@eng.hokudai.ac.jp
†isuemune@es.hokudai.ac.jp

[1] J. Nagamatsu *et al.*, Nature (London) **410**, 63 (2001).
[2] T. Kamihara *et al.*, J. Am. Chem. Soc. **130**, 3296 (2008).
[3] *Quantum Computation and Quantum Information*, edited by M. A. Nielsen and I. L. Chuang (Cambridge University Press, Cambridge, England, 2000).
[4] J. Johansson *et al.*, Phys. Rev. Lett. **96**, 127006 (2006).
[5] J. E. Mooij *et al.*, Science **285**, 1036 (1999).
[6] A. O. Niskanen *et al.*, Science **316**, 723 (2007).
[7] J. Clarke *et al.*, Nature (London) **453**, 1031 (2008).
[8] R. McDermott *et al.*, Science **307**, 1299 (2005).
[9] R. Sobolewski *et al.*, IEEE Trans. Appl. Supercond. **13**, 1151 (2003).
[10] *Superconductivity of Metals and Alloys*, edited by P. G. de Gennes (Westview Press, Oxford, UK, 1999).
[11] *Theory of Superconductivity*, edited by J. R. Schrieffer (Westview Press, Oxford, UK, 1971).
[12] E. Hamanura, Phys. Status Solidi B **234**, 166 (2002).
[13] *Principles of Superconductive Devices and Circuits*, edited by T. van Duzer and C. W. Turner (Prentice Hall PTR, Upper Saddle River, USA, 1999).
[14] A. J. Bennett *et al.*, Phys. Rev. B **72**, 033316 (2005).
[15] The measured Nb T_C is slightly lower than the intrinsic value of 9.3 K. This is due to fluctuating evaporation conditions of the Nb metal and changes slightly depending on samples.
[16] Y. Hayashi *et al.*, Appl. Phys. Express **1**, 011701 (2008).
[17] I. Suemune *et al.*, Appl. Phys. Express **3**, 054001 (2010).
[18] I. Suemune *et al.*, Jpn. J. Appl. Phys. **45**, 9264 (2006).
[19] Y. Asano *et al.*, Phys. Rev. Lett. **103**, 187001 (2009).
[20] R. K. Ahrenkiel *et al.*, Appl. Phys. Lett. **72**, 3470 (1998).
[21] T. Akazaki *et al.*, J. Appl. Phys. **66**, 6121 (1989).
[22] I. Vurgaftman *et al.*, J. Appl. Phys. **89**, 5815 (2001).